Accurate and Efficient Proximity Effect Correction for Electron Beam Lithography Based on Distributed Parallel Computing

Haojie Zhao
College of Electrical and Information Engineering
Hunan University
Changsha, China
haojie_zhao@hnu.edu.cn

Wenze Yao
College of Electrical and Information Engineering
Hunan University
Changsha, China
wenzeyao@hnu.edu.cn

Hongcheng Xu
College of Electrical and Information Engineering
Hunan University
Changsha, China
hongchengxu@hnu.edu.cn

Siyuan Zhang
College of Electrical and Information Engineering
Hunan University
Changsha, China
siyuanzhang0103@hnu.edu.cn

Yujie Yang
College of Electrical and Information Engineering
Hunan University
Changsha, China
yujieyang2426@hnu.edu.cn

Xin Zhang
College of Electrical and Information Engineering
Hunan University
Changsha, China
zhangxin2302@hnu.edu.cn

Jie Liu
College of Electrical and Information Engineering
Hunan University
Changsha, China
jie_liu@hnu.edu.cn

2022 International Workshop on Advanced Patterning Solutions (IWAPS) | 979-8-3503-9766-6/22/$31.00 ©2022 IEEE | DOI: 10.1109/IWAPS57146.2022.9972245

Abstract*— This paper proposes an efficient proximity effect correction (PEC) method for electron beam lithography (EBL) based on distributed parallel computing. To facilitate PEC calculations of large-scale layout, this method splits the exposure layout into multiple sub-layouts, and distributes them to different computer nodes for calculation through the message passing interface (MPI) technology. Under the premise of ensuring accuracy of PEC of the same layout, compared to the calculation time of 1 computing node (56 CPU cores per node), the acceleration ratios using N_{node}=2, 4 and 6 nodes are N_{ratio}=2.28, 5.29, and 8.31, respectively. Given the same PEC calculation case with N_{pixel} pixels, when N_{node} is increased, the number of pixels calculated by one node ($n=N_{pixel}/N_{node}$) decreases, leading to $N_{ratio}/N_{node}>1$ due to the $O(n\times log(n))$ time complexity of the fast Fourier transform (FFT) in convolution computation. The proposed distributed parallelization scheme has been implemented in the second version of the HNU-EBL software (http://www.ebeam.com.cn/).

Keywords—electron beam lithography, proximity effect correction, distributed parallel computing, MPI, FFT

I. INTRODUCTION

Electron beam lithography (EBL) is a high-precision maskless direct-write lithography technology for micro-nano patterning [1-3]. Proximity effect (PE) of electron beam lithography (EBL) is a phenomenon caused by the scattering of the incident electrons with the resist and substrate. The PE leads to distorted energy deposition in the exposed layout, which will seriously affect the lithography pattern quality. Proximity effect correction (PEC) methods [4-6] optimize target layout by modifying layout exposure dose or pattern shape. As the critical dimension (CD) size of the layout is further reduced, the amount of computation used to calculate the PEC will increase dramatically. When calculating a large-sized exposure layout, it is difficult to meet the computational efficiency requirements using one computing node. Therefore, it is necessary to explore a PEC method based on multi-node parallelization.

This paper proposes an efficient PEC method for EBL based on distributed parallel computing. The energy deposition calculation of the layout is the most time-consuming part of the PEC method. The fast Fourier transform (FFT) convolution is often used to calculate convolution for two-dimensional layouts [7]. After overlapping processing, large-sized target layouts are split and distributed to different computing nodes through the message passing interface (MPI) technology [8]. Different nodes are responsible for the FFT calculation of a certain area, and finally these sub-areas are integrated into the result layout. The accuracy and efficiency of the proposed method have been verified by experiments. In addition, the parallel computing module based on the supercomputing platform has been integrated to the HNU-EBL software [9-11].

In section II, the PEC method based distributed parallel computing is detailed. In section III, the accuracy and efficiency of the proposed method are verified. In section IV, HNU-EBL software is introduced. In section V, a summary is made.

II. MODEL AND METHOD

In the section, we present PEC method for EBL based on distributed parallel computing. In Section II.A, the error of our proposed method is obtained by analyzing the evaluation of layout energy deposition. In Section II.B, the steps of our proposed method are described.

A. Energy Deposition Analysis

The Monte Carlo method [12] can be used to simulate the energy distribution of electrons in the resist and the substrate, and can be fitted with several forms of Gaussian functions [13, 14]. In this paper, without loss of generality, the double Gaussian function

$$P(r)=\frac{K}{\pi(1+\eta)}\left(\frac{1}{\alpha^2}\exp\left(-\frac{r^2}{\alpha^2}\right)+\frac{\eta}{\beta^2}\exp\left(-\frac{r^2}{\beta^2}\right)\right) \quad (1)$$

979-8-3503-9766-6/22/$31.00 ©2022 IEEE

Authorized licensed use limited to: HUNAN UNIVERSITY. Downloaded on December 13,2022 at 07:08:07 UTC from IEEE Xplore. Restrictions apply.

is used as the point spread function (PSF), where α, β represent the range of forward scattering and back scattering, respectively, and η is the ratio of the energy intensity of the forward scattering and back scattering, K is a constant.

The energy deposition distribution after exposure can be obtained by convolving PSF with the layout exposure dose as

$$E(\boldsymbol{r})=\iint P(|\boldsymbol{r}-\boldsymbol{r}'|)\sigma(\boldsymbol{r}')\mathrm{d}\boldsymbol{r}' \tag{2}$$

where $E(\boldsymbol{r})$ is the energy deposition located at the layout $\boldsymbol{r}=(x, y)$; $\sigma(\boldsymbol{r}')$ is the exposure dose is the energy deposition located at the layout $\boldsymbol{r}'=(x', y')$.

The desired energy deposition position is the origin of the coordinate axis (i.e., $\boldsymbol{r}=(0, 0)$). The effect region of the layout dose distribution is $[-d, d]\times[-d, d]$. The energy deposition contribution E_d in this effect region is

$$\begin{aligned} E_d=\frac{K}{\pi(1+\eta)}\Bigg(&\int_{-d}^{d}\int_{-d}^{d}\frac{1}{\alpha^2}\exp\left(-\frac{x^2+y^2}{\alpha^2}\right)\sigma(x, y)\,\mathrm{d}x\mathrm{d}y \\ &+\eta\int_{-d}^{d}\int_{-d}^{d}\frac{1}{\beta^2}\exp\left(-\frac{x^2+y^2}{\beta^2}\right)\sigma(x, y)\mathrm{d}x\mathrm{d}y\Bigg) \end{aligned} \tag{3}$$

The upper limit e of the energy deposition error at the origin can be obtained as [15]

$$e=\frac{4K\sigma_{max}}{1+\eta}\left(\left(1-\Phi\left(\frac{\sqrt{2}d}{\alpha}\right)\right)^2+\eta\left(1-\Phi\left(\frac{\sqrt{2}d}{\beta}\right)\right)^2\right) \tag{4}$$

where σ_{max} is the maximum value of the layout dose distribution; the normal distribution function $\Phi(x)$ is

$$\Phi(x)=\frac{1}{\sqrt{2\pi}}\int_{-\infty}^{x}\exp\left(-\frac{t^2}{2}\right)\mathrm{d}t \tag{5}$$

In the above analysis, the energy deposition in our method only evaluates the influence of part of the layout, which can meet the error requirements. Note that the above precision analysis can be extended to other forms of PSF.

B. Distributed Parallel Computing Method

The proposed method consists of three main steps:

***Step* (1)** Import GDSII layout and splits the exposure layout into multiple sub-layouts. Each computing node reads a part of the layout and gets the coordinates of all element vertices. According to the size of the layout and the number of computing nodes, the target layout is divided into multiple sub-layouts with m rows and n columns. Each computing node will perform PEC on a sub-layout. Therefore, computing nodes need to exchange the layout information read before, so that each computing node has all the information of a sub-layout. As shown in Fig. 1 (a), the layout information possessed by the computing nodes P_i and P_j are represented in blue and red, respectively. The computing node P_i needs to send the information of the elements in the black dashed box to P_j, and then the layout information owned by the computing nodes P_i and P_j is shown in Fig. 1 (b). Finally, each computing node has all the information of a sub-layout.

***Step* (2)** Computing nodes communication and sub-layout energy deposition evaluation**.** As shown in Fig. 2 (a), the edge information of adjacent sub-layout is exchanged via MPI non-blocking communication interfaces *MPI_Irecv* and *MPI_Isend*. And d can be determined according to the PSF parameter and Eq. (4). Then each computing node has all the information of the sub-layout owned by itself, including the edge information of adjacent sub-layout. To exploit the overlap of computation and communication, while sending and receiving data using the MPI non-blocking interface, the pre-computation data is prepared using in subsequent computations for energy deposition. In Fig. 2 (a), the computing node P_i receives the sub-layout edge information owned by the computing nodes P_{i-n-1}, P_{i-n}, P_{i-n+1}, P_{i-1}, P_{i+1}, P_{i+n-1}, P_{i+n}, and P_{i+n+1} as grey area. And the range of the layout data owned by the node P_i is shown in the black dashed box shown in Fig. 2 (b). Finally, the energy deposition of the current sub-layout can be calculated using the FFT by

$$E(\boldsymbol{r}_i)=\sum_{j=1}^{N}P(|\boldsymbol{r}_i-\boldsymbol{r}_j|)\sigma(\boldsymbol{r}_j) \tag{6}$$

where $E(\boldsymbol{r}_i)$ is the energy deposition at the exposure point located at layout $\boldsymbol{r}_i$, $\sigma(\boldsymbol{r}_j)$ is the exposure dose at the exposure point at layout $\boldsymbol{r}_j$, N is the number of exposure points of the layout. Eq. (6) is the discretized form of Eq. (2).

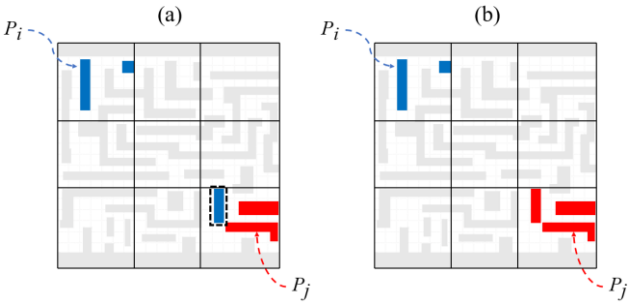

Fig. 1 (a), (b) represent the layout data owned by computing nodes P_i and P_j before and after exchanging information, respectively.

After calculating the layout energy deposition, the development process was simulated using a threshold development model.

$$H(\boldsymbol{r})=\begin{cases}0, & E(\boldsymbol{r})<E_{\mathrm{thr}}\\ 1, & E(\boldsymbol{r})\geq E_{\mathrm{thr}}\end{cases} \tag{7}$$

where E_{thr} is a threshold value related to the resist dissolution, $H(\boldsymbol{r})$ is the layout shape after development. The quality of the developed layout can be quantified by the mean square error (MSE) defined as

$$\mathrm{MSE}=\frac{\sum_{i=1}^{N}(H(\boldsymbol{r}_i)-D(\boldsymbol{r}_i))^2}{N} \tag{8}$$

where $D(\boldsymbol{r})$ is the target development contour of the layout.

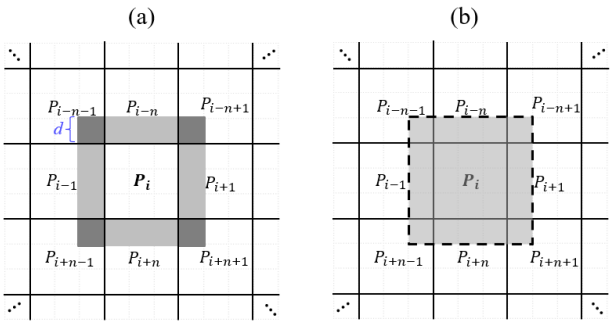

Fig. 2 (a) the adjacent computing nodes of P_i need to send the edge of the sub-layout they own to P_i, (b) P_i finally has all the information about the layout inside the dotted box.

Authorized licensed use limited to: HUNAN UNIVERSITY. Downloaded on December 13,2022 at 07:08:07 UTC from IEEE Xplore. Restrictions apply.

***Step* (3)** Dose correction. When MSE is less than the preset error limit ε, the PEC is completed. Otherwise, the layout dose distribution needs to be updated, and iterated from ***Step* (2)** to ***Step* (3)** until MSE is less than the preset error limit ε. The dose distribution $\sigma(\boldsymbol{r})$ is updated using the state-of-the-art iterative method and more details can be found in [16, 17].

$$\sigma_k(\boldsymbol{r})=\frac{D_T\sigma_{k-1}(\boldsymbol{r})}{E(\boldsymbol{r})} \tag{9}$$

where $\sigma_k(\boldsymbol{r})$ is the input dose for the k-th iteration, D_T is the target energy deposition and ε is a preset constant.

III. Result

In this section, we describe the results from numerical experiments that demonstrate the scalability of our method for different layout sizes and the accuracy under different computer nodes.

(1) PSF parameter. The HNU-EBL software integrates the Monte Carlo method to simulate the redistribution of the energy caused by the scattering of the electron beam in the resist and the substrate. The PSF is obtained by fitting the redistributed energy with a double Gaussian function. In this experiment, the double Gaussian PSF shown in Eq. (1) is used, where α=14.982 nm, β=197.479 nm, η=1.6593, K =25.0363. Note that the proposed method is applicable to other PSF models.

(2) Machines. The main scalability results have been obtained that each compute node have two Intel(R) Xeon(R) Gold 6258R CPU @ 2.70GHz processor with 56 cores and 192 GB memory.

(3) Implementations and libraries. The algorithms were implemented in C++ using the MPI and FFTW libraries and accelerated with Open Multiprocessing (OpenMP) [18].

(4) Scalability tests. The scalability results are reported in Fig. 3. In our experiments, the size of the layout is N_{pixel} =2.88, 3.34, 3.84, 4.30, 4.80, $\times 10^9$ pixels, and the number of computing nodes is N_{node}=1, 2, 4, and 6, respectively. Under the premise of ensuring accuracy of PEC of the same layout, compared to the calculation time of 1 computing node (56 CPU cores per node), Fig. 3 (a) shows that when the number of computing nodes is fixed, the computing time increases linearly with the layout size. Fig. 3 (b) shows that when the layout size is fixed, the computing time is inversely proportional to the number of computing nodes, and the acceleration ratios is linearly related to the number of computing nodes. The acceleration ratios using N_{node}=2, 4 and 6 nodes are N_{ratio}=2.28, 5.29, and 8.31, respectively. Given the same PEC calculation case with N_{pixel} pixels, when N_{node} is increased, the number of pixels calculated by one node (n=N_{pixel}/N_{node}) decreases, leading to N_{ratio}/N_{node}>1 due to the $O(n\times log(n))$ time complexity of the fast Fourier transform (FFT) in convolution computation.

(5) Accuracy tests. The accuracy results are reported in Fig. 4. The size of the layout is N_{pixel}=2.57×10^7 pixels, and the number of computing nodes is N_{node}=1, 2, 4, 6, and 9, respectively. The Fig. 4 (a), (b), (c), and (d) represent the relative errors that computing nodes is N_{node}=2, 4, 6, and 9, respectively. In the implementation of our proposed method, the width of the sub-layout edge region is d=4.5×$\beta/\sqrt{2}$, i.e., d=628. Thus, the theoretical e is about 10^{-11}. When the single-precision data type is used in the proposed method, our computational accuracy will be guaranteed. Fig. 4 shows that the maximum relative error e is about 1×10^{-5}, indicating that our proposed distributed parallel algorithm is extremely accurate.

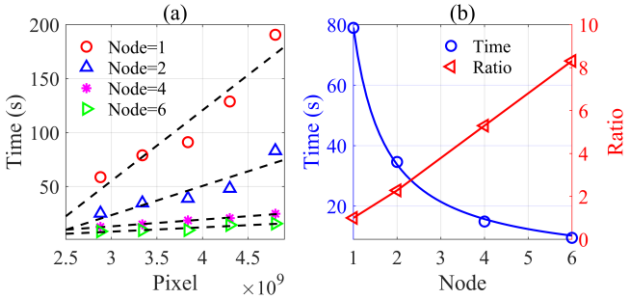

Fig. 3 (a) In the case of several different nodes, the calculation time consumption is with the change curve of the number of pixels. (b) For a test benchmark layout, the speedup ratios under different node cases are analyzed.

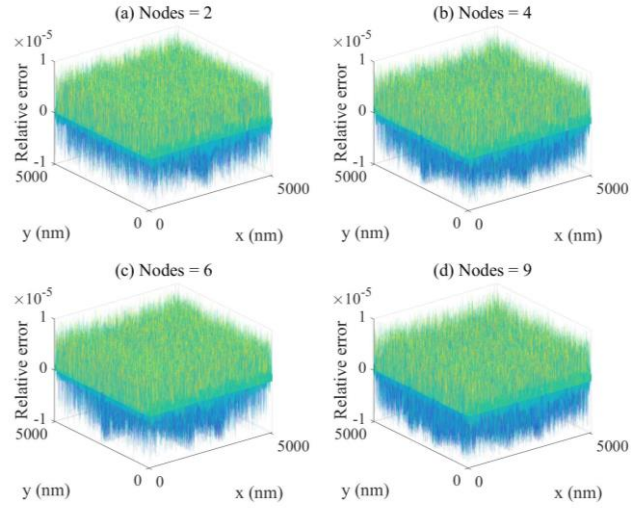

Fig. 4 The relative error distribution between the multi-computing node and the single-computing node PEC results. (a), (b), (c), and (d) represent the relative errors that computing nodes is N_{node}=2, 4, 6, and 9 on the PEC of the same layout, respectively.

IV. Software

The PEC method based on distributed parallel computing has been integrated to the HNU-EBL software, developed by Hunan University. For more details of the HNU-EBL software, please refer to http://www.ebeam.com.cn/.

As shown in Fig. 5, after the function "Using Supercomputer" is checked and the relevant parameters are entered, the computing task can be submitted to the supercomputing platform. Note that user needs to log in before using this function. As shown in Fig. 6, after submitting computing task, user can update computing task status, cancel computing task and download the PEC results file in the user interface.

Authorized licensed use limited to: HUNAN UNIVERSITY. Downloaded on December 13,2022 at 07:08:07 UTC from IEEE Xplore. Restrictions apply.

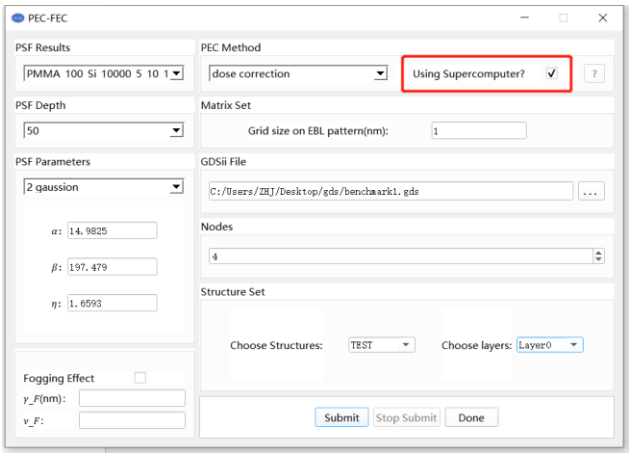

Fig. 5 Schematic diagram of PEC task submission interface based on distributed parallel computing.

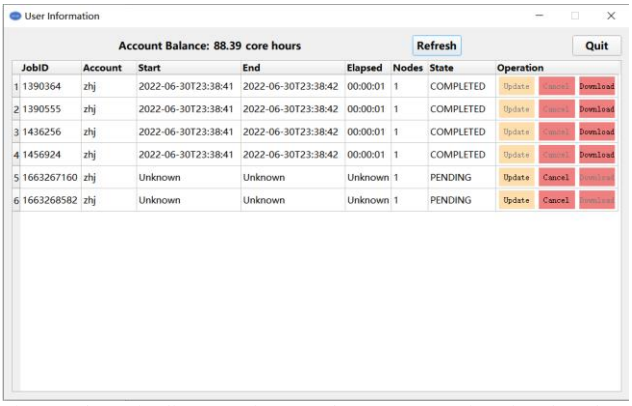

Fig. 6 Schematic diagram of user task management interface based on supercomputing platform.

V. CONCLUSION

This paper proposes a PEC method for EBL based on distributed parallel computing. The proposed method breaks through the limitation of computing memory and time for the PEC of super-large layouts. The experiment result shows that compared with the traditional single-node computing method, the acceleration ratios using N_{node}=2, 4 and 6 nodes (56 CPU cores per node) are N_{ratio}=2.28, 5.29, and 8.31 under the premise of ensuring the calculation accuracy.

ACKNOWLEDGMENT

This work is supported by the National Natural Science Foundation of China (#61804049); the Fundamental Research Funds for the Central Universities of P.R. China; Huxiang High Level Talent Gathering Project (#2019RS1023); the Key Research and Development Project of Hunan Province, P.R. China (#2019GK2071); the Technology Innovation and Entrepreneurship Funds of Hunan Province, P.R. China (#2019GK5029); the Fund for Distinguished Young Scholars of Changsha (#kq1905012); the National Natural Science Foundation of China (#62101182).

REFERENCES

[1] B. Sun, P. Zhang, T. Zhang, S. Shangguan, S. Wu, and X. Ma, "Single step electron-beam lithography archiving lift-off for T-gate in high electron mobility transistor fabrication," *Microelectronic Engineering,* vol. 229, p. 111337, 2020.

[2] H. Wei, D. Yunhui, Z. Lianqing, and D. Mingli, "Angular sensing system based on Y-type twin-core fiber and reflective varied-line spacing grating fabricated by electron beam lithography," *Results in Physics,* vol. 18, p. 103193, 2020.

[3] J. Zheng *et al.*, "30 GHz surface acoustic wave transducers with extremely high mass sensitivity," *Applied Physics Letters,* vol. 116, no. 12, p. 123502, 2020.

[4] B. D. Cook and S.-Y. Lee, "PYRAMID-a hierarchical, rule-based approach toward proximity effect correction. II. Correction," *IEEE Transactions on Semiconductor Manufacturing,* vol. 11, no. 1, pp. 117-128, 1998.

[5] C.-H. Liu, P.-L. Tien, P. C. Ng, Y.-T. Shen, and K.-Y. Tsai, "Model-based proximity effect correction for electron-beam direct-write lithography," in *Alternative Lithographic Technologies II*, 2010, vol. 7637: SPIE, pp. 430-437.

[6] E. H. Eriksen *et al.*, "Dose regularization via filtering and projection: An open-source code for optimization-based proximity-effect-correction for nanoscale lithography," *Microelectronic Engineering,* vol. 199, pp. 52-57, 2018.

[7] M. E. Haslam, J. F. McDonald, D. C. King, M. Bourgeois, D. G. L. Chow, and A. J. Steckl, "Two - dimensional Haar thinning for data base compaction in Fourier proximity correction for electron beam lithography," *Journal of Vacuum Science & Technology B: Microelectronics Processing and Phenomena,* vol. 3, no. 1, pp. 165-173, 1985.

[8] W. Gropp, W. D. Gropp, E. Lusk, A. Skjellum, and A. D. F. E. E. Lusk, *Using MPI: portable parallel programming with the message-passing interface*. MIT press, 1999.

[9] C. Hou, W. Yao, W. Liu, Y. Chen, H. Duan, and J. Liu, "Ultrafast and Accurate Proximity Effect Correction of Large-Scale Electron Beam Lithography based on FMM and SaaS," in *2020 International Workshop on Advanced Patterning Solutions (IWAPS)*, 2020: IEEE, pp. 1-3.

[10] W. Liu *et al.*, "HNU-EBL: A Software Toolkit for Electron Beam Lithography Simulation and Optimization," in *2021 International Workshop on Advanced Patterning Solutions (IWAPS)*, 2021: IEEE, pp. 1-4.

[11] W. Yao *et al.*, "Efficient Proximity Effect Correction Using Fast Multipole Method with Unequally Spaced Grid for Electron Beam Lithography," *IEEE Transactions on Computer-Aided Design of Integrated Circuits and Systems,* 2022.

[12] J. Zhou and X. Yang, "Monte Carlo simulation of process parameters in electron beam lithography for thick resist patterning," *Journal of Vacuum Science & Technology B: Microelectronics and Nanometer Structures Processing, Measurement, and Phenomena,* vol. 24, no. 3, pp. 1202-1209, 2006.

[13] S. Wind, M. Rosenfield, G. Pepper, W. Molzen, and P. Gerber, "Proximity correction for electron beam lithography using a three - Gaussian model of the electron energy distribution," *Journal of Vacuum Science & Technology B: Microelectronics Processing and Phenomena,* vol. 7, no. 6, pp. 1507-1512, 1989.

[14] F. Koba, H. Yamashita, and H. Arimoto, "Highly accurate proximity effect correction for 100 kV electron projection lithography," *Japanese journal of applied physics,* vol. 44, no. 7S, p. 5590, 2005.

[15] T. Abe and T. Takigawa, "Proximity effect correction for high - voltage electron beam lithography," *Journal of applied physics,* vol. 65, no. 11, pp. 4428-4434, 1989.

[16] T. R. Groves, "Efficiency of electron-beam proximity effect correction," *Journal of Vacuum Science & Technology B: Microelectronics and Nanometer Structures Processing, Measurement, and Phenomena,* vol. 11, no. 6, pp. 2746-2753, 1993.

[17] J. J. Zarate and H. Pastoriza, "Correction algorithm for the proximity effect in e-beam lithography," in *2008 Argentine School of Micro-Nanoelectronics, Technology and Applications*, 2008: IEEE, pp. 38-42.

[18] X.-M. Pan, W.-C. Pi, and X.-Q. Sheng, "On OpenMP parallelization of the multilevel fast multipole algorithm," *Progress In Electromagnetics Research,* vol. 112, pp. 199-213, 2011.

Authorized licensed use limited to: HUNAN UNIVERSITY. Downloaded on December 13,2022 at 07:08:07 UTC from IEEE Xplore. Restrictions apply.